ADVANCES IN NUCLEAR SCIENCE AND APPLICATIONS

Volume 1, No. 1 (2025), P. 40-49

Improvement of standard ceramic technology for producing YTZP ceramics using hydrothermal synthesis

Y.A. Garanin[1,2], M.R. Issenov[2], B.A. Baraban[2], A.A. Mitashev[2]

[1]L.N. Gumilyov Eurasian National University, Astana, Kazakhstan

[2]Institute of Nuclear Physics, Almaty, Kazakhstan

e-mail: garanin_ua_1@enu.kz

Received: 22 January 2025

Abstract

Yttria-stabilized tetragonal zirconia polycrystal (YTZP) ceramics are widely used due to their excellent mechanical properties, corrosion resistance, and biocompatibility. Conventional YTZP production involves multiple processing stages, but using hydrothermally synthesized $ZrO_2-Y_2O_3$ nanoparticles as the starting material can simplify the process. In this study, $ZrO_2-Y_2O_3$ nanoparticles were synthesized hydrothermally from $ZrO(NO_3)_2 \cdot 2H_2O$ and $Y(NO)_3 \cdot 2H_2O$ at 1300°C for 12 hours. X-ray diffraction and Raman spectroscopy confirmed an exclusively c-ZrO_2 phase. TEM analysis showed nanosized spherical conglomerates (4-14 nm), while TGA indicated residual synthesis byproducts. Short-term thermal exposure at 1300°C promoted Y^{3+} incorporation into the ZrO_2 lattice, forming the tetragonal-ZrO_2 (t-ZrO_2) phase. The bulk ceramic sample exhibited 50% volume shrinkage and high porosity due to byproduct evaporation. The final composition consisted of 99% t-ZrO_2 and <1% monoclinic-ZrO_2 (m-ZrO_2). Using hydrothermally synthesized nanoparticles eliminated several conventional processing steps, including mixing, grinding, and preliminary annealing, streamlining YTZP ceramics production.

Introduction

The development of modern technologies in the field of developing new types of catalysts, semiconductors, heat-resistant protective coatings, etc. requires the creation of new types of material. Ceramic materials based on metal oxides have long established themselves as promising materials in the areas listed above [1, 2, 3, 4, 5]. Among the wide variety of oxide ceramics, zirconium dioxide (ZrO_2) stands out due to its exceptional mechanical and corrosion resistance, chemical inertness, and ability to withstand significant thermal loads, making it widely used in various industries and technologies [6, 7]. In addition, ZrO_2 nanoparticles exhibit enhanced catalytic activity, making them useful as catalysts [8]. The main factor that stopped the mass use of ZrO_2-based ceramics was phase transformations during heating to relatively high temperatures and subsequent cooling. Under standard conditions, ZrO_2 has a monoclinic structure (m-ZrO_2), which transforms into a tetragonal structure (t-ZrO_2) upon heating to 1200^0C. This transformation involves a significant expansion of the lattice parameter, leading to cracking and destruction in bulk samples [9]. Further heating to 2370^0C leads to a phase transition from the tetragonal phase to the cubic phase (c-ZrO_2) [10]. Meanwhile, the tetragonal and cubic phases exhibit the most interesting mechanical and electrical properties, as well as chemical inertness and high-temperature stability. The primary approach to addressing phase instability is doping ZrO_2 with varying concentrations of yttrium (Y^{3+}), cerium (Ce^{4+}), magnesium (Mg^{2+}), and calcium (Ca^{2+}) ions. Due to their different valences and ionic radii compared to Zr, these dopants help stabilize the desired phase [11, 12, 13, 14]. One of the most popular options is doping ZrO_2 with Y^{3+} ions (YTZP ceramics). By introducing a relatively low dopant concentration (5 mol.%), t-ZrO_2 can be fully stabilized, preventing reverse phase transformations under prolonged thermal and mechanical loads.

Another approach to obtaining high-temperature ZrO_2 phases stable under normal conditions is the synthesis of particles smaller than 10–20 nm. ZrO_2 nanoparticles have high surface energy, resulting in the generation of numerous oxygen vacancies and defects, which ultimately stabilize high-temperature phases under normal conditions [6]. This method for obtaining high-temperature ZrO_2 phases offers the advantage of producing nanoparticles with excellent size homogeneity, which significantly influences volume shrinkage and porosity during ceramic synthesis from the resulting powders. At present, ZrO_2 nanoparticles are obtained by chemical vapor deposition, coprecipitation, sol-gel, spray pyrolysis and hydrothermal methods [15, 16]. By adjusting the parameters of hydrothermal synthesis—such as temperature, synthesis duration, solution acidity, and the concentration and type of starting materials—the shape, surface morphology, size, and phase composition of the particles can be controlled. This makes the method one of the most promising for producing metal oxide nanoparticles [17]. The main disadvantage of the hydrothermal method for synthesizing ZrO_2 particles is their temperature instability. Many studies report that when ZrO_2 nanoparticles are heated above 600^0C, a phase transformation from t(c)-ZrO_2 to m-ZrO_2 occurs due to the particle size exceeding the threshold for t(c)-ZrO_2 stability [17, 18]. It can be assumed that simultaneous hydrothermal synthesis of ZrO_2 and Y_2O_3 nanoparticles enables the doping of ZrO_2 with Y^{3+} ions. As a result, the issue of temperature instability in t(c)-ZrO_2 nanoparticles can be resolved, while the excellent homogeneity of the nanoparticles allows for the production of low-porosity ceramics, simplifying the overall technological process. One of the most popular methods for synthesizing oxide ceramics is standard ceramic technology, which includes the following stages: mixing and grinding of the starting materials; preliminary annealing of samples and their grinding; introduction of a plasticizer and preparation of press blanks; high-temperature annealing. By using nanoparticles obtained through the hydrothermal method as starting materials, the processes of powder mixing and milling, plasticizer addition, as well as pre-sintering followed by milling can be eliminated. This is due to the nanoscale size of the particles and the ability to stabilize the desired high-temperature phase in the initial state.

Despite the considerable amount of research on the hydrothermal synthesis of $\mathrm{ZrO_2}$ nanoparticles, there is a lack of studies focused on synthesizing bulk ceramic samples from these nanoparticles and subsequently investigating their properties. In article [19], the authors synthesized 8YTZP ceramics and concluded that the hydrothermal synthesis of $\mathrm{ZrO_2 - Y_2O_3}$ nanoparticles has several advantages for their further use as a precursor in the production of bulk YTZP ceramic samples. However, they also note several disadvantages of this method. In particular, the high tendency of nanoparticles to agglomerate leads to the formation of a coarse-grained microstructure. At the same time, Song et al. [20] synthesized 5YTZP ceramics using nanoparticles obtained by the hydrothermal method and achieved a sufficiently dense ceramic with a submicron grain size. However, the synthesis process involves a multi-step technology, including nanoparticle crystallization, grinding of agglomerates, and pre-annealing. Therefore, it is necessary to further explore the feasibility of synthesizing bulk ceramic samples from $\mathrm{ZrO_2}$ nanoparticles obtained by the hydrothermal method.

1 Methods and materials

$\mathrm{ZrO_2 - Y_2O_3}$ nanoparticles were obtained by hydrothermal synthesis in a 25 ml steel autoclave with a Teflon liner. A 0.1 mol/L solution of zirconium (4) oxonitrate dihydrate $(\mathrm{ZrO(NO_3)_2 \cdot 2H_2O})$ with a volume of 17.5 ml with the addition of 5 mol% Yttrium (3) nitrate hydrate $(\mathrm{Y(NO)_3 \cdot 2H_2O})$ was used as the starting material. 5 ml of 1 mol/l NaOH solution was used as a mineralizer. The starting material and mineralizer were mixed in a Teflon liner to obtain a solution pH of 10. The synthesis was carried out in a drying oven at a temperature of 130^0C for 12 hours. To purify the obtained powder from unwanted synthesis products, centrifugation was carried out in distilled water at a speed of 6000 rpm for 4 cycles of five minutes, after which the obtained powder was dried for 5 hours at a temperature of 60^0C.

Ceramic samples in the form of tablets were obtained using standard ceramic technology, including:1) production of press blanks using a press with a pressure of 430 MPa; 2) two-stage annealing of press blanks at temperatures of 400 and 1600^0C for 1 and 5 hours, respectively, in a Nabertherm LHT 08/18 furnace (Nabertherm GmbH, Lilienthal, Germany) with a heating rate of $10^0C/min$. Before and after annealing, the geometric parameters and mass of all samples were measured in order to determine the parameters of apparent density and volumetric shrinkage.

X-ray phase analysis of the synthesized powders and bulk ceramic samples of $\mathrm{ZrO_2{-}Y_2O_3}$ was performed by X-ray diffraction on a Rigaku SmartLab diffractometer with $\mathrm{CuK\alpha}$ X-ray radiation in Bragg-Brentano geometry. The size of the coherent scattering region (CSR) was calculated for the main reflections ((111) monoclinic phase and (101) tetragonal ((111) cubic) phase of ZrO_2) using the Scherrer equation [19]:

$$d_{XRD} = \frac{0.9\lambda}{\beta\cos\theta}. \tag{1}$$

where β is the full width at half maximum (FWHM) for each of the reflections; 0.9 is a coefficient taking into account the shape of the particles.

The calculation of the proportion of the monoclinic phase in the samples was carried out using the equation [20]:

$$X_m = \frac{I_m(\bar{1}11) + I_m(111)}{I_m(\bar{1}11) + I_m(111) + I_m(101)}, \tag{2}$$

where I_m, I_t are the intensities of the reflections on the diffraction pattern.

In addition, the phase composition of the samples was investigated by Raman spectroscopy using an Enspectr M532 spectrometer (Spectr-M LLC, Chernogolovka, Russia) with a laser wavelength of 532 nm. Heat-induced mass loss analysis was performed using thermogravimetric analysis (TGA) on a Themys One instrument (Setaram KEP Technology, Caluire, France). The sample was heated in an argon atmosphere with a partial pressure of 0.5 MPa to 1000^0C at a rate of $10^0C/min$. The sizes and morphology of nanoparticles were investigated by transmission electron microscopy (TEM) using a Jeol JEM – 1400Plus transmission electron microscope (Jeol, Tokyo, Japan). The surface morphology and grain size of the ceramic samples, as well as the elemental composition, were investigated using scanning electron microscopy (SEM) on a Phenom ProX G6 microscope (Thermo Fisher Scientific, Eindhoven, The Netherlands).

2 Results

The results of X-ray diffraction of the synthesized sample are shown in Figure 1. From the obtained data it follows that the sample is characterized by the presence of exclusively c-ZrO_2 (PDF 01-071-6425) with space group Fm-3m (225) or t-ZrO_2 (PDF 00-050-1089) with space group P42/nmc(137). It can be assumed that the absence of reflections characteristic of Y_2O_3 is due to several reasons: 1) Y_2O_3 particles were incorporated into the ZrO_2 lattice during synthesis; 2) The X-ray diffractometer did not detect the small amount of Y_2O_3; 3) Y_2O_3 particles are amorphous. Using the Scherrer equation, the value of the coherent scattering region, which characterizes the minimum particle size, was calculated to be 6 nm, which indirectly confirms the nanosize of $ZrO_2 - Y_2O_3$ particles. Meanwhile, due to the very similar crystal structure of cubic and tetragonal ZrO_2, it is almost impossible to reliably determine which phase (cubic or tetragonal) is present in the sample using X-ray diffraction. The Raman spectroscopy method allows to exactly separate the cubic and tetragonal phases of ZrO_2. The inset in Figure 1 presents Raman spectroscopy data, where a broad mode in the range of 500–600 cm^{-1}, characteristic of the cubic ZrO_2 phase, can be observed. This indicates the absence of tetragonal and monoclinic ZrO_2 phases and is consistent with the data obtained by X-ray diffraction. It can also be stated that the stabilization of ZrO_2 by Y_2O_3 particles did not occur during the hydrothermal synthesis, as this concentration should have led to the stabilization of the tetragonal ZrO_2 phase. It is known that the stabilization of high-temperature ZrO_2 phases is possible even without the introduction of dopants due to the high surface energy of nanoparticles. In this case, the key requirement is a particle size of less than 20–10 nm [6]. Based on the above, it can be concluded that the stabilization of the cubic phase occurred due to the nanoscale size of the particles rather than the introduction of a dopant in the form of Y_2O_3 particles. Additionally, the Raman spectrum exhibits modes around $1056, 1345$, and 1608 cm^{-1}, which can be attributed to the presence of $NaNO_3$ in the synthesized powder, as well as a mode in the range of 3000–3700 cm^{-1}, which can be associated with OH groups.

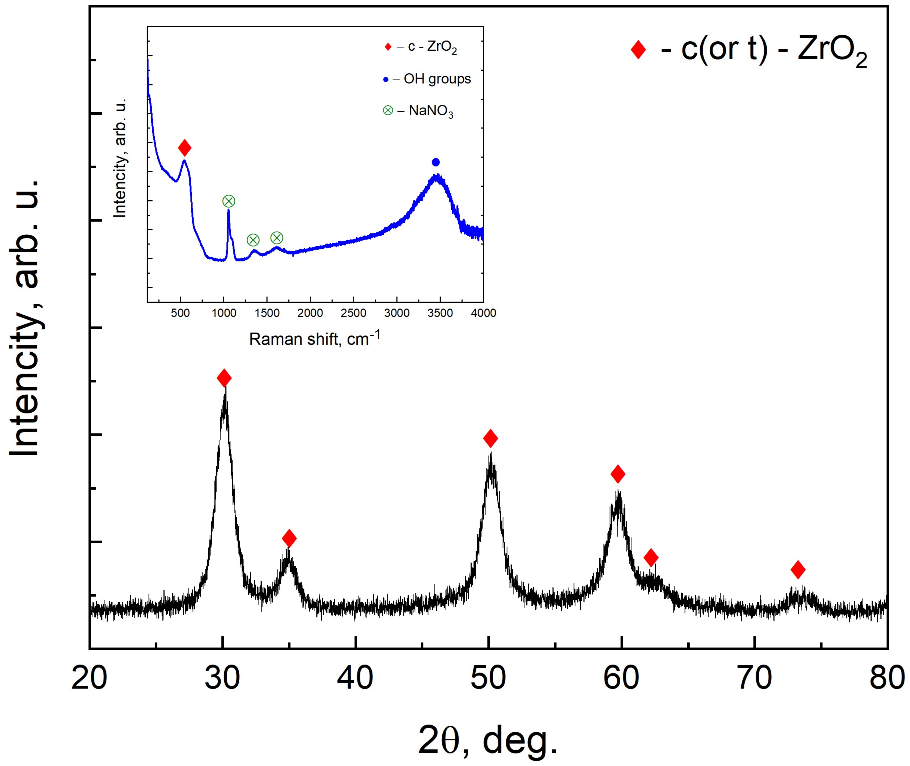

Figure 1: Results of X-ray diffraction of $ZrO_2 - Y_2O_3$ nanoparticles obtained by hydrothermal synthesis. The inset shows the Raman spectrum of the same sample

To study the particle size and morphology, TEM images of the synthesized $ZrO_2 - Y_2O_3$ particles were obtained and are shown in Figure 2. It can be seen that the size of the obtained particles is in the range of 5–14 nm with the highest content of particles in the region of 4–7 nm, which confirms the RCD data obtained using the Scherrer equation, and the particles themselves have a spherical shape.

One of the fundamental conditions in the production of hard protective ceramic products is the low porosity of the final product. During hydrothermal synthesis, due to their high surface energy, nanoparticles absorb water and residual synthesis products on their surface. Upon heating, these absorbed substances evaporate, becoming one of the main causes of pore formation. To determine the proportion of residual synthesis products, present in the synthesized $ZrO_2 - Y_2O_3$ powders, a study was conducted using the TGA method. From Figure 3 it can be seen that when heating particles to 1000 ^0C, a loss of $4.5 - 5\,\%$ of the mass of the original amount is observed. The mass loss in the sample can be divided into 4 regions. In the first region (up to 200^0C), physically adsorbed water evaporates; In the second

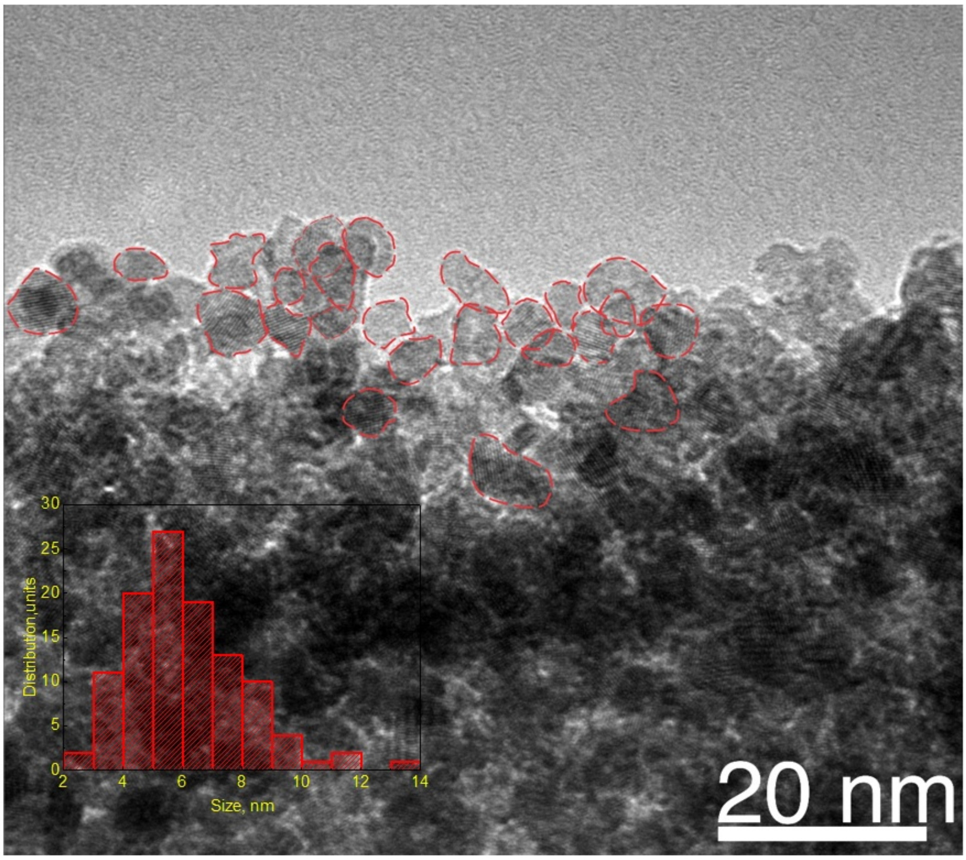

Figure 2: TEM images of $ZrO_2 - Y_2O_3$ nanoparticles obtained by hydrothermal synthesis; inset: Particle size distribution.

region (200–400 ^0C), chemically adsorbed water is removed; In the third region (400–600 ^0C), hydroxide groups decompose and are eliminated; In the fourth region, residual synthesis by-products decompose [21].

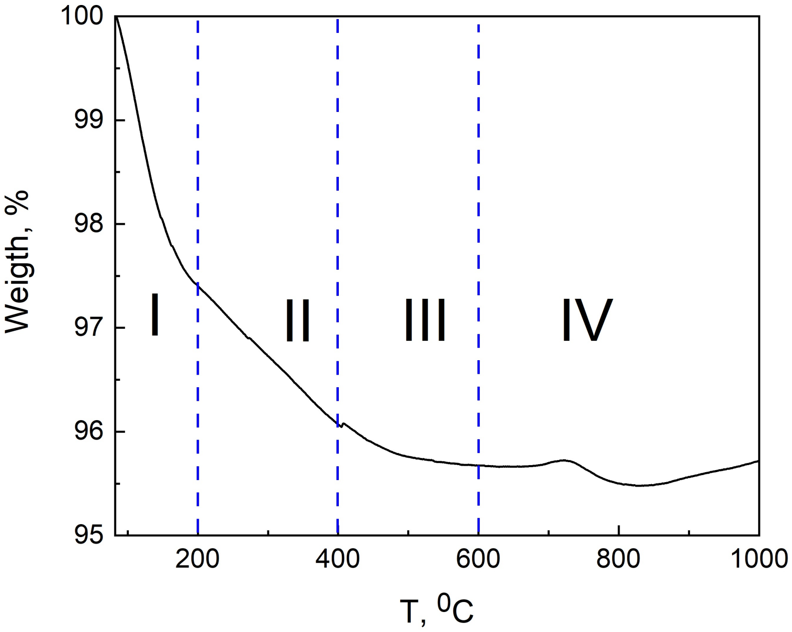

Figure 3: TGA results for the $ZrO_2 - Y_2O_3$ sample

In the next step, the synthesized samples of $ZrO_2 - Y_2O_3$ nanoparticles were subjected to short-term thermal annealing at a temperature of 1300 ^0C (the temperature of the phase transition $\mathrm{m} - ZrO_2 \rightarrow t - ZrO_2$) for 15 minutes. As a result, the appearance of the monoclinic phase ZrO_2 (PDF 00-065-0687) space group P21/a(14)) (17 %) and the tetragonal phase ZrO_2 (PDF 00-050-1089) with space group P42/nmc(137) (83 %) can be observed. The decrease in the full width at half maximum (FWHM) of the peaks in the obtained diffraction pattern indicates an increase in the average particle size, which leads to a phase transition of the $\mathrm{c} - ZrO_2 \rightarrow \mathrm{m} - ZrO_2$ type. Thus, even with short thermal annealing, the stabilization of t-ZrO_2 occurs due to the partial incorporation of Y^{3+} ions into the ZrO_2 lattice. The inset to Figure 4 shows a Raman spectrum that shows modes at 147, 262, 317 cm^{-1}, which are characteristic of $\mathrm{t} - ZrO_2$, and modes at 178, 198, 221, 305, 335, 348, 382, 475,504, 538, 563, 619, 637 cm^{-1}, which are characteristic of $\mathrm{m} - ZrO_2$.

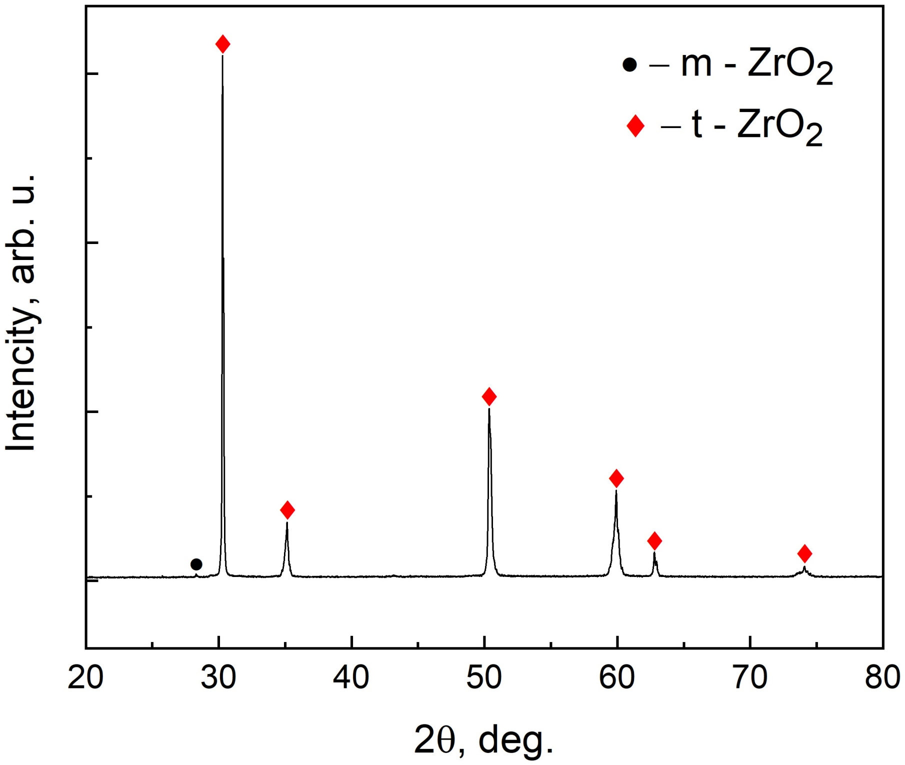

Figure 4: Results of X-ray diffraction of the $ZrO_2 - Y_2O_3$ sample after annealing at 1300 ^0C for 15 minutes

The next stage of the research was the synthesis of bulk ceramic samples from the obtained nanoparticles. Figure 5 shows X-ray diffraction data for a bulk sample obtained using standard ceramic technology. The obtained sample is characterized by the presence of t - ZrO_2 phase (PDF 00-050-1089) with space group P42/nmc(137) and an insignificant content (less than 1 %) of m - ZrO_2 phase (PDF 00-065-0687) space group P21/a(14). As mentioned earlier, this fact is due to the incorporation of Y^{3+} ions into the ZrO_2 crystal lattice as a result of thermal exposure during annealing and, as a consequence, the stabilization of the t - ZrO_2 phase after cooling. A significant reduction in the proportion of the m-ZrO_2 phase, in contrast to short-term temperature annealing, is associated with the completion of doping processes as a result of exposure to a higher temperature and a significantly longer annealing time. The small values of the FWHM peaks in the diffraction pattern compared to the data of the original samples indicate a significant increase in the particle size as a result of their sintering into larger conglomerates and the formation of a grain structure.

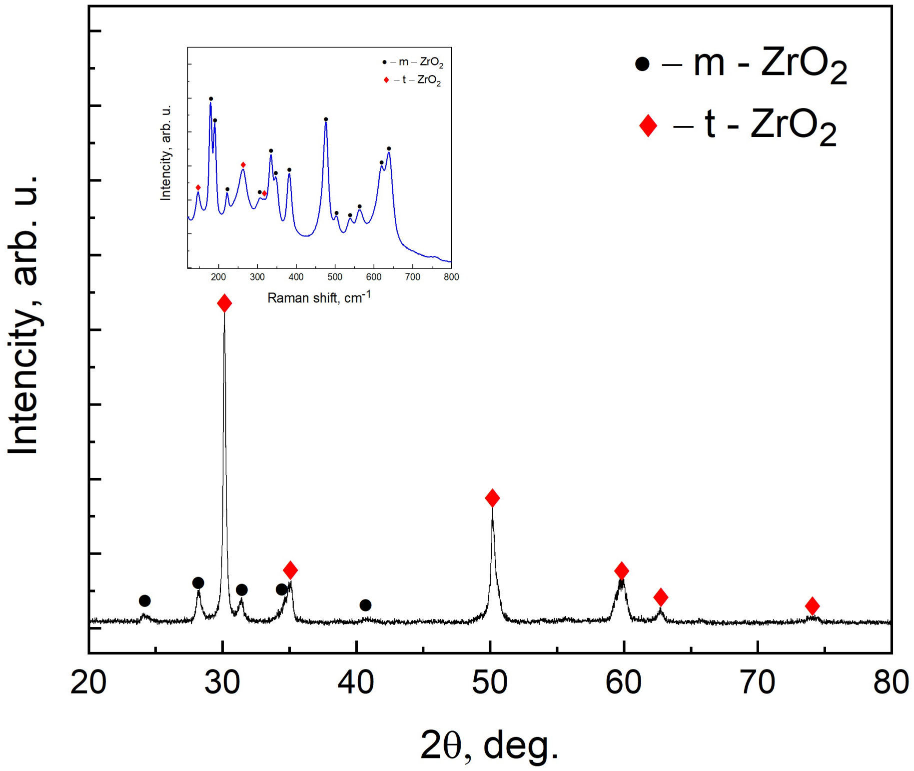

Figure 5: Results of X-ray diffraction of a bulk ceramic sample of $\mathrm{ZrO_2-Y_2O_3}$ after annealing at a temperature of 1600 ^0C for 5 hours

From the SEM images obtained, it can be observed that despite the large values of volumetric shrinkage (50 %) calculated by measuring the geometric dimensions of the sample before and after sintering, the synthesized ceramic is characterized by the presence of a large number of macro- and micropores, with a calculated density of 5.2 g/cm^3, which is 85 % of the theoretical density (6 g/cm^3). This fact is due to the content of water and residual synthesis products in the original powders, which evaporate upon heating and serve as a source of pore formation. It is assumed that to reduce the porosity of the sample, the synthesized nanoparticles need to be pre-annealed. The synthesized $\mathrm{ZrO_2-Y_2O_3}$ ceramic is characterized by the presence of grains ranging in size from 1 to 6 μm and 10 to 20 μm. However, it should be noted that despite the large number of small grains, the volumetric fraction of grains 10 μm and larger is significantly higher.

Analysis of the elemental composition showed that the obtained ceramics do not contain any impurity elements that could remain as residual products after hydrothermal synthesis and consist exclusively of oxygen (67 at. %), Zirconium (30 at. %) and Yttrium (3 at. %).

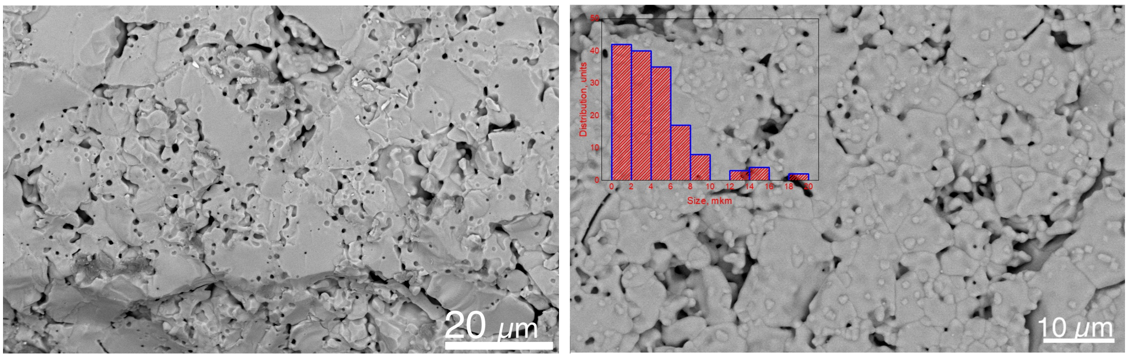

Figure 6: SEM images of (left) a chip and (right) the surface of a bulk sample of $ZrO_2 - Y_2O_3$ ceramics after annealing at a temperature of 1600^0C for 5 hours

Conclusions

In this article, $ZrO_2 - Y_2O_3$ nanoparticles were obtained by hydrothermal synthesis. Using the X-ray diffraction method, it was established that the obtained $ZrO_2 - Y_2O_3$ particles are characterized by the presence of exclusively $c(t) - ZrO_2$ phase with a coherent scattering region size of 6 nm. Using Raman spectroscopy, it was reliably established that the sample contains the $c - ZrO_2$ phase. It can be assumed that the absence of peaks characteristic of Y_2O_3 in the diffraction patterns and Raman spectra is associated with their amorphous nature or their incorporation into the ZrO_2 lattice. However, the main driving factor for the stabilization of the $c - ZrO_2$ phase is the nanosize of the synthesized particles, which is confirmed by TEM data and is consistent with generally accepted literature data. TGA showed that nanoparticles lose 5–6 % of their initial mass when heated to 1000 ^0C, which is due to the content of water and residual synthesis products in the sample. With short-term temperature exposure, phase transformations of the type $c - ZrO_2 \rightarrow m - ZrO_2 \rightarrow t - ZrO_2$ occur, caused by: 1) an increase in the average particle size to values above 20 nm; 2) the incorporation of Y^{3+} ions into the ZrO_2 crystal lattice. During the synthesis of bulk ceramics from $ZrO_2 - Y_2O_3$ nanoparticles, significant shrinkage (50 %) is observed, but the ceramics are characterized by the presence of a large number of macro- and micropores, the formation of which is associated with the evaporation of water sorbed on the surface. However, by using the co-synthesis of $ZrO_2 - Y_2O_3$ particles by the hydrothermal method, it is possible to exclude several stages from the standard ceramic technology, namely: grinding and mixing of the initial powders, production of the press powder and preliminary annealing. Thus, the further development of ceramic synthesis technology based on $ZrO_2 - Y_2O_3$ nanoparticles obtained by the hydrothermal method can be considered promising.

References

[1] G. Vekinis, M. F. Ashby, and P. W. R. Beaumont, Acta Metall. Mater. **38**, 1151 (1990).

[2] L. Fu *et al.*, Mater. Sci. Eng. A **840**, 142904 (2022).

[3] A. Nevárez *et al.*, Dent. Mater. J. **35**, 392 (2016).

[4] X. Q. Cao, R. Vassen, and D. Stoever, J. Eur. Ceram. Soc. **24**, 1 (2004).

[5] J. Liu, G. Li, and J. Wu, Mater. Chem. Phys. **258**, 123894 (2021).

[6] A. K. Chitoria, A. Mir, and M. A. Shah, Ceram. Int. **49**, 32343 (2023).

[7] J. R. Kelly and I. Denry, Dent. Mater. **24**, 289 (2008).

[8] I. Fatimah *et al.*, Inorg. Chem. Commun. **143**, 109808 (2022).

[9] G. K. Bansal and A. H. Heuer, Acta Metall. **20**, 1281 (1972).

[10] J. Li *et al.*, Sci. China Ser. E **51**, 1858 (2008).

[11] T. Wen *et al.*, Curr. Appl. Phys. **39**, 133 (2022).

[12] Y. Ling *et al.*, Ceram. Int. **48**, 10547 (2022).

[13] X. Zhu *et al.*, Ceram. Int. **50**, 14718 (2024).

[14] A. Kumar, P. Kumar, and A. S. Dhaliwal, J. Korean Ceram. Soc. **59**, 370 (2022).

[15] N. Tabassum *et al.*, Mater. Today Commun. **26**, 102156 (2021).

[16] M. Mosavari, A. Khajehhaghverdi, and R. Mehdinavaz Aghdam, Inorg. Chem. Commun. **157**, 111293 (2023).

[17] L. Liu *et al.*, Ceram. Int. **48**, 32649 (2022).

[18] N. Kumari *et al.*, Nanoscale Adv. **4**, 4210 (2022).

[19] G. Dell'Agli and G. Mascolo, Solid State Ion. **160**, 363 (2003).

[20] J. Song *et al.*, J. Alloys Compd. **856**, 156766 (2021).

[21] C. J. Szepesi and J. H. Adair, J. Am. Ceram. Soc. **94**, 4239 (2011).

[22] H. Toraya, M. Yoshimura, and S. Somiya, J. Am. Ceram. Soc. **67**, C119 (1984).

[23] Y. Garanin *et al.*, Sci. Rep. **14**, 29398 (2024).